

South Dakota State University  
**Open PRAIRIE: Open Public Research Access Institutional  
Repository and Information Exchange**

---

GSCE Faculty Publications

Geospatial Sciences Center of Excellence (GSCE)

---

12-2014

# A Cross Comparison of Spatiotemporally Enhanced Springtime Phenological Measurements From Satellites and Ground in a Northern U.S. Mixed Forest

Liang Liang  
*University of Kentucky*


Mark D. Schwartz  
*University of Wisconsin - Milwaukee*

Zhuosen Wang  
*University of Massachusetts Boston*

Feng Gao  
*USDA, Agricultural Research Service*

Crystal B. Schaaf  
*University of Massachusetts Boston*

Follow us for additional works at: [http://openprairie.sdstate.edu/gsce\\_pubs](http://openprairie.sdstate.edu/gsce_pubs)

 Part of the [Climate Commons](#), [Environmental Sciences Commons](#), [Physical and Environmental Geography Commons](#), [Remote Sensing Commons](#), and the [Spatial Science Commons](#)

---

## Recommended Citation

Liang, Liang; Schwartz, Mark D.; Wang, Zhuosen; Gao, Feng; Schaaf, Crystal B.; Tan, Bin; Morisette, Jeffrey T.; and Zhang, Xiaoyang, "A Cross Comparison of Spatiotemporally Enhanced Springtime Phenological Measurements From Satellites and Ground in a Northern U.S. Mixed Forest" (2014). *GSCE Faculty Publications*. Paper 13.  
[http://openprairie.sdstate.edu/gsce\\_pubs/13](http://openprairie.sdstate.edu/gsce_pubs/13)

This Article is brought to you for free and open access by the Geospatial Sciences Center of Excellence (GSCE) at Open PRAIRIE: Open Public Research Access Institutional Repository and Information Exchange. It has been accepted for inclusion in GSCE Faculty Publications by an authorized administrator of Open PRAIRIE: Open Public Research Access Institutional Repository and Information Exchange. For more information, please contact [michael.biondo@sdstate.edu](mailto:michael.biondo@sdstate.edu).

---

**Authors**

Liang Liang, Mark D. Schwartz, Zhuosen Wang, Feng Gao, Crystal B. Schaaf, Bin Tan, Jeffrey T. Morisette, and Xiaoyang Zhang

# A Cross Comparison of Spatiotemporally Enhanced Springtime Phenological Measurements From Satellites and Ground in a Northern U.S. Mixed Forest

Liang Liang, Mark D. Schwartz, Zhuosen Wang, Feng Gao, Crystal B. Schaaf, *Member, IEEE*, Bin Tan, Jeffrey T. Morisette, and Xiaoyang Zhang

**Abstract**—Cross comparison of satellite-derived land surface phenology (LSP) and ground measurements is useful to ensure the relevance of detected seasonal vegetation change to the underlying biophysical processes. While standard 16-day and 250-m Moderate Resolution Imaging Spectroradiometer (MODIS) vegetation index (VI)-based springtime LSP has been evaluated in previous studies, it remains unclear whether LSP with enhanced temporal and spatial resolutions can capture additional details of ground phenology. In this paper, we compared LSP derived from 500-m daily MODIS and 30-m MODIS–Landsat fused VI data with landscape phenology (LP) in a northern U.S. mixed forest. LP was previously developed from intensively observed deciduous and coniferous tree phenology using an upscaling approach. Results showed that daily MODIS-based LSP consistently estimated greenup onset dates at the study area (625 m × 625 m) level with 4.48 days of mean absolute error (MAE), slightly better than that of using 16-day standard VI (4.63 days MAE). For the observed study areas, the time series with increased number of observations confirmed that post-bud burst deciduous tree phenology contributes the most to vegetation reflectance change. Moreover, fused VI time series demonstrated closer correspondences with LP at the community level (0.1–20 ha) than using MODIS alone at the study area level (390 ha). The fused LSP captured greenup onset dates for respective forest communities of varied sizes and compositions with four days of the overall MAE. This study supports further use

of spatiotemporally enhanced LSP for more precise phenological monitoring.

**Index Terms**—Daily Moderate Resolution Imaging Spectroradiometer (MODIS), Earth Observing System (EOS) land validation core sites, landscape phenology (LP), land surface phenology (LSP), phenology, Spatial and Temporal Adaptive Reflectance Fusion Model (STARFM).

## I. INTRODUCTION

**P**HENOLOGY studies the life-cycle timing of organisms and is a sensitive indicator of the condition and variability of biosphere–atmosphere interactions [1], [2]. Remotely sensed land surface phenology (LSP, see Table VI for a list of acronyms used in this paper) provides multitemporal seasonal vegetation change information at regional to global scales [3], [4]. Accurately monitoring LSP is crucial for tasks such as climate change impact assessment [5], [6], forest disturbance surveillance [7], [8], agricultural and socioeconomic analyses [4], [9], and ecosystem matter/energy exchange modeling [10], [11]. However, akin to most remote sensing measurements, the accuracy of LSP is limited by the spatial and temporal resolutions of sensor/platform systems and is subject to additional glitches from sensor systematic errors, atmospheric path radiance contaminations, and surface reflectance biases [12]–[15]. Therefore, ground validation is essential for gauging the level of accuracy in satellite-based phenological monitoring and for linking LSP parameters to specific phenological processes [16]–[19].

Most LSP products are derived from time series of vegetation index [VI, e.g., Normalized Difference Vegetation Index (NDVI) and Enhanced Vegetation Index (EVI)] time series, which are based on data collected by polar orbiting satellite borne sensors such as the Advanced Very High Resolution Radiometer (AVHRR) since 1980s [20] and the Moderate Resolution Imaging Spectroradiometer (MODIS) since 2000s [21]. The relatively coarse spatial resolution (250 m to 1 km) and the large temporal compositing windows [8–16 days, for filtering cloud contamination with a maximum value composite (MVC) approach] of the standard VI products [22] have allowed very limited spatiotemporal detail that can be henceforth used for deriving LSP metrics (e.g., onset of greenup and browning) [23], [24]. The greenup onset derived from MODIS data

Manuscript received June 23, 2013; revised January 22, 2014 and March 10, 2014; accepted March 15, 2014. Date of publication April 17, 2014; date of current version June 12, 2014. This work was supported in part by the National Science Foundation under Grant BCS-0649380 and Grant BCS-0703360 and in part by the National Aeronautics and Space Administration under Grant NNX12AL38G.

L. Liang is with the Department of Geography, University of Kentucky, Lexington, KY 40506-0027 USA (e-mail: liang.liang@uky.edu).

M. D. Schwartz is with the Department of Geography, University of Wisconsin-Milwaukee, Milwaukee, WI 53201-0413 USA.

Z. Wang is with the School for the Environment, University of Massachusetts Boston, MA 02125-3393 USA. He is also with the Terrestrial Information Systems Laboratory, NASA Goddard Space Flight Center, Greenbelt, MD 20771 USA, and also with the NASA Postdoctoral Program, Oak Ridge Associated Universities, Oak Ridge, TN 37831 USA.

F. Gao is with the Hydrology and Remote Sensing Laboratory, USDA Agricultural Research Service, Beltsville, MD 20705-2350 USA.

C. B. Schaaf is with the School for the Environment, University of Massachusetts, Boston, MA 02125-3393 USA.

B. Tan is with the NASA Goddard Space Flight Center, Sigma Space Corporation, Greenbelt, MD 20771 USA.

J. T. Morisette is with the U.S. Geological Survey, North Central Climate Science Center, Colorado State University, Fort Collins, CO 80525 USA.

X. Zhang is with the Geospatial Sciences Center of Excellence, South Dakota State University, Brookings, SD 57007 USA.

Digital Object Identifier 10.1109/TGRS.2014.2313558

estimates the time when vegetated landscapes such as deciduous forests [25] and agricultural fields [26], [27] start to turn green in spring. However, most *in situ* phenological records are available only for plant individuals at discrete locations, missing areal representativeness that is comparable to satellite pixels [28], with the exception of a high-resolution phenology dataset used in our previous study [19]. These limitations make it challenging to derive statistically meaningful comparisons between satellite- and ground-based phenology products.

Efforts to reconcile the scale mismatch between *in situ* and coarse-resolution remote sensing phenology observations have taken either a satellite downscaling approach or a ground up-scaling approach. Fisher *et al.* [29] and Fisher and Mustard [30] utilized annual time series composited from multiyear Landsat data to facilitate downscaling of MODIS (8-day, 500 m) phenology to 30-m resolution for a closer comparison with ground data. Liang and Schwartz [31] and Liang *et al.* [19] developed an upscaling approach to generate landscape phenology (LP) representations based on intensively collected *in situ* data [32] in order to validate standard MODIS (16-day, 250 m) VI-based LSP. A clear linkage between greenup onset and deciduous tree leaf bud burst timing was found. Additionally, validation work has been also done using field measurements by tower-based spectrometers and webcams [33], [34]. These studies suggested a general agreement between coarse-resolution LSP greenup estimates with the spring phenology of temperate deciduous canopies.

This study is a follow-up effort of the validation work documented in Liang *et al.* [19]. The rationale of this study is to ascertain whether spatiotemporally enhanced LSP products could capture additional details of ground processes. Especially with the higher temporal and spatial resolution VI time series becoming available, new opportunities are emerging for improved LSP detection. In particular, VI derived from the MODIS Bidirectional Reflectance Distribution Function (BRDF) and albedo products (MCD43) [35], [36] reduce biases from surface reflectance anisotropy from using the standard VI product (MOD13). Daily MODIS BRDF/albedo products are now processed to retain more usable temporal information to capture rapidly changing surface conditions [37], [38]. Furthermore, fusion algorithms have been developed to synergize the spatial and temporal resolutions of multiple sensor data for more detailed land surface biophysical characterization [39], [40]. Specifically, Gao *et al.* [41] developed a Spatial and Temporal Adaptive Reflectance Fusion Model (STARFM) to blend the more frequent (i.e., daily) temporal information from MODIS and finer (i.e., 30 m) spatial information from Landsat for applications that require both increased temporal and spatial resolutions. Ju *et al.* [42] applied temporally complete daily MODIS nadir-view BRDF-adjusted reflectance (NBAR) NDVI time series for phenology monitoring. Such spatially and temporally enhanced remote sensing products are promising for LSP analysis with increased details [43], [44] and warrant the need for additional ground validation.

Very limited attempts at validating the fused satellite-data-based LSP have been made [45], [46] due to the lack of spatially and temporally compatible field observations. Bhandari *et al.* [45] pointed out the need for intensive field information similar

to that used in our previous study [19] to effectively evaluate the fused time series. The high-resolution *in situ* phenology data collected in a northern U.S. mixed forest (as used in our previous study) provide a unique opportunity to address this need. Moreover, in our previous validation effort targeting coarse-resolution MODIS LSP, the potential of this field dataset was not fully exploited. In this paper, we performed a cross comparison between the springtime LSP from daily MODIS NBAR and MODIS–Landsat fused VI time series and corresponding LP derived previously from our intensive ground phenological observation. We hypothesize that LSP with enhanced spatiotemporal resolutions is useful for more precise remote sensing detection of vegetation phenology.

## II. DATASETS AND METHODS

### A. Ground Phenology Observation and Scaling

The field phenological observations were conducted in a spatially and temporally intensive setting. Two 625 m  $\times$  625 m study areas were established in the vicinity of the Park Falls/WLEF flux tower (45.94,  $-90.27$ ) located within the Chequamegon–Nicolet National Forest, northern Wisconsin (see Fig. 1). The two study areas represent, respectively, a maple-pine-dominated forest patch (north) and a more mixed aspen-fir-dominated forest patch (south). The size of each study area was initially chosen to cover an area comparable with a 500 m  $\times$  500 m MODIS pixel with consideration of sampling design and limited resources. The forest is mostly a mixed second growth with dominant deciduous species including trembling aspen (*Populus tremuloides*), sugar maple (*Acer saccharum*), red maple (*Acer rubrum*), and speckled alder (*Alnus rugosa*), and dominant coniferous species such as balsam fir (*Abies balsamea*), red pine (*Pinus resinosa*), and white cedar (*Thuja occidentalis*). Among the coniferous trees, only balsam fir showed observable spring phenology (new needle cluster development). A cyclic sampling scheme [47] was adopted, and a total of 288 plots with 888 trees were sampled.

Tree phenology observation followed a continuous buds-to-leaves protocol quantifying leaf development through *buds visible* (100), *buds swollen* (200), *buds open* (leaves or candles visible, 300), *leaf clusters/candles out* (not fully unfolded, 400), and *leaves/needles fully unfolded* (500) [32]. Percentage ranges as specified by respective scores (0%–10% [0], 10%–50% [10], 50%–90% [50], and 90%–100% [90]) were used to further estimate the proportion within a given canopy that had reached a certain developmental stage. For instance, a tree canopy with estimated 10%–50% of buds open would be attributed with a score of 310. Beyond the leaf unfolding stage, an additional *leaf expansion* (600) level was used for deciduous canopy phenology with a slightly different percentage breakdown according to leaf size (< 25% of full [0], 25%–50% [25], 50%–75% [50], and > 75% [75]). Phenological observations were conducted by observers with the help of binoculars at a bidaily frequency over four to five weeks (from approximately late April to late May) during the time of growing season onset. In this paper, we included data collected for the two complete 625 m  $\times$  625 m study areas in 2008 and 2009, as well as data from 2006 and 2007 for an initial, geographically smaller study area of 625 m  $\times$  275 m.

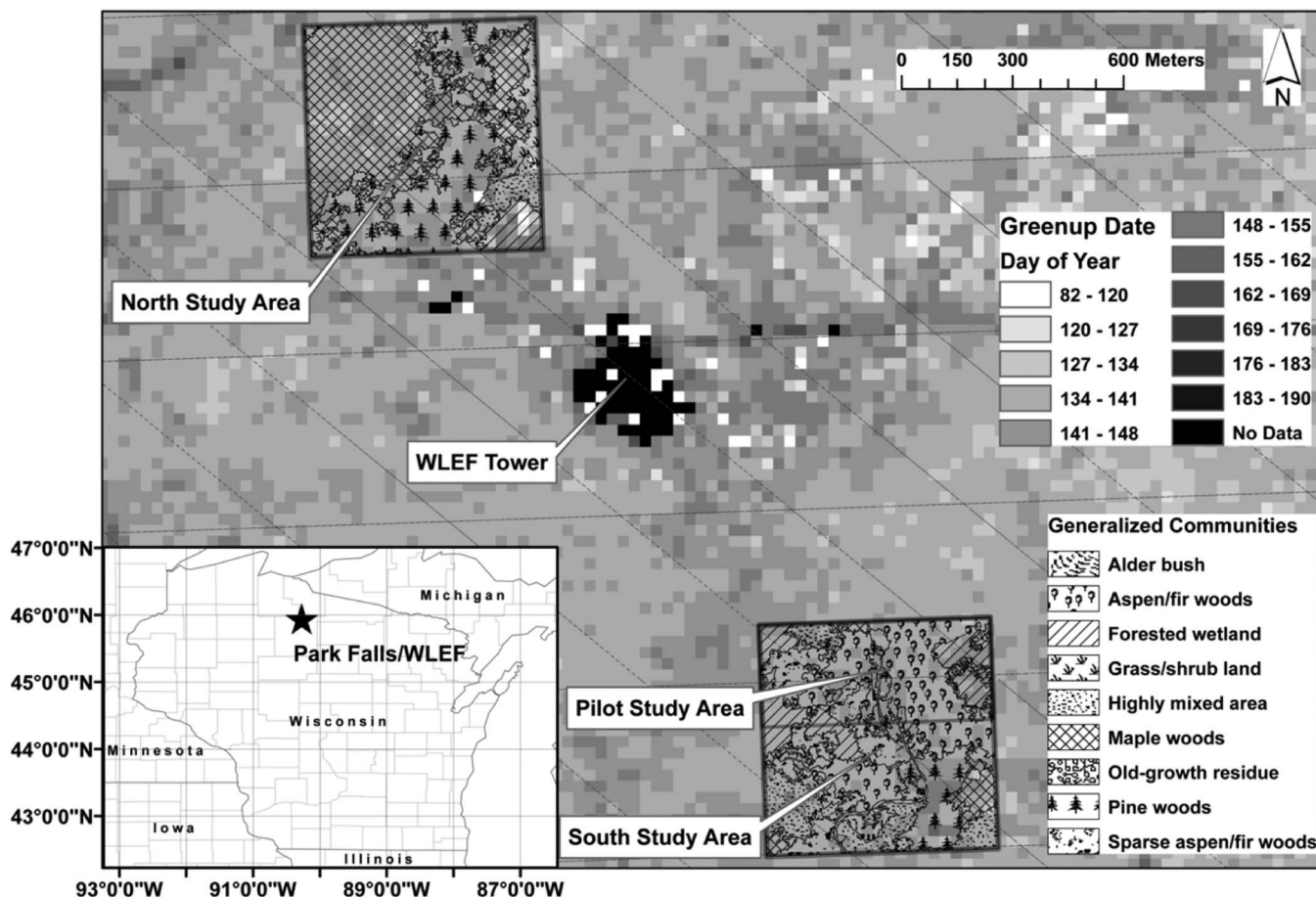


Fig. 1. Study site location (inset map) and diagram of study area layout. The study areas and generalized community distribution are overlaid upon fused Landsat (EVI, 2008) greenup onset date estimates. The 500-m MODIS NBAR pixel grid is shown as parallelograms under the UTM (15 N) projection.

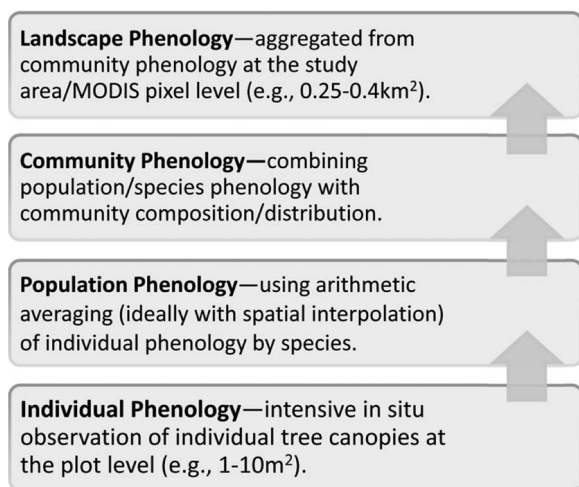


Fig. 2. Diagram showing the concept and steps of scaling intensively conducted *in situ* phenological observations up to the landscape level. A previously published figure showing more technical details of this scaling process is available in [19, Fig. 2].

Scaling up tree phenology observations followed an ecologically coherent and nested hierarchical process (see Fig. 2; cf. Fig. 1). First, individual canopy phenology was aggregated to the population level using an arithmetic averaging of all observations by species in each study area. Population-level

phenology was then combined into community phenology with community compositions estimated from subpixel spectral unmixing of a pair of 2.4-m multispectral leaf-on/leaf-off QuickBird (operated by DigitalGlobe) images for separating the portions of the deciduous, coniferous, and bare soil within each pixel. Furthermore, study-area-level LP was produced by aggregating community phenology with additional community distribution information derived from supervised image segmentation of a 1-m pan-sharpened IKONOS (operated by GeoEye, now merged into DigitalGlobe) image. The IKONOS image with slightly higher spatial resolution than QuickBird was used to obtain a better discrimination of community boundaries. Two types of LP index were then produced: 1) specific LP indices retaining field phenology protocol inference and dimension as aggregated for deciduous and coniferous trees separately, and 2) an integrated LP index mimicking satellite VI. The integrated LP index was produced by accounting for the differential surface reflectance contributions of deciduous and coniferous phenology, respectively, with specified weights (determined using QuickBird NDVI change of pure deciduous/coniferous forest stands). Both specific and integrated LP indices were available for the entire study areas, as well as respective forest communities, and were used to compare with LSP at both the study area and community levels. Additional technical details on field data collection and LP indices derivation are available in [32] and [19].

TABLE I  
USABLE DATES (DOY 81–230) OF 16-DAY MODIS STANDARD VI PRODUCTS AND DAILY MODIS NBAR DATASETS (INCLUDED ALL CLOUD-FREE DATA FOR OUR STUDY AREAS) FOR THE NORTH AND SOUTH STUDY AREAS (2008 AND 2009), RESPECTIVELY

		16-day composite MODIS standard VI products		Daily MODIS NBAR	
		Usable day of year	Total	Usable day of year	Total
2008	North	89, 111*, 121, 144, 149, 165, 185, 194, 224	9	89, 94, 114, 121, 126-128, 135, 142, 144, 148, 149, 159, 165, 169-171, 182, 187, 190, 193, 194, 196, 205, 208-210, 215, 224, 227, 228	31
	South	94, 111*, 121, 144, 149, 165, 183, 194, 215	9	89, 114, 118, 121, 126-128, 135, 141, 142, 144, 148, 149, 159, 165, 169-171, 182, 183, 187, 190, 193, 194, 196, 197, 205, 209, 210, 215, 223, 228	32
2009	North	89*, 105, 118, 142, 155, 171, 187, 194, 215*	9	88, 96-98, 100-102, 105-107, 113, 118, 134, 138, 139, 142-145, 148, 150, 154, 155, 163, 164, 166, 171, 174, 176, 177, 187, 190, 192-194, 224	37
	South	89*, 105, 118, 142, 155, 171, 187, 194, 215*	9	88, 96-98, 100-102, 105-107, 113, 118, 138, 139, 142-145, 148, 150, 154, 155, 163, 166, 171, 174, 176, 177, 187, 190, 192-194, 216, 224	35

\*indicates that average from multiple dates across the study area was used.

### B. MODIS Daily NBAR VI

The MODIS BRDF and albedo products (MCD43) have been in production for more than a decade using the first 7 MODIS band reflectances from both Terra and Aqua satellites [35]. The standard Collection V005 8-day product makes use of a linear “kernel-driven” RossThick-LiSparse Reciprocal (RTLSR) BRDF model to describe the reflectance anisotropy of each pixel at a 500-m gridded resolution. The MODIS BRDF/albedo 1-day mode of the product emphasizes the daily observation in an attempt to capture rapidly changing surface conditions. Daily BRDF/albedo products have been implemented as a Direct Broadcast algorithm and have become the standard product in the upcoming Collection V006 reprocessing of the MODIS archive. Cloud-contaminated pixels that were flagged in the MODIS surface reflectance products were excluded. All cloud-free data were incorporated in the daily products without void interpolation, rendering maximum temporal resolution available for a location as limited only by local weather conditions. In this paper, a magnitude inversion is performed by using the latest daily full inversions developed with 16 days of valid observations as the priori information for the next succeeding day for BRDF application [37], [38]. Thus, the LSP at the study area level was based on VI derived from the daily MODIS NBAR data.

We used the 500-m daily MODIS NBAR VI time series extending from day of year (DOY) 81 (late March) to 230 (late August) of each year from 2006 to 2009. This specified time window covered the entire spring season as well as late winter and summer growing season peak as boundary conditions for curve fitting. The daily MODIS NBAR time series tripled the number of useable/cloud-free images for our study areas in comparison to 16-day MVC products (see Table I). However, approximately 80% (75%–79%) of the daily images were still affected by cloud cover or aerosols at our study site and therefore rendered useless. The greenup onset dates were generated using the logistic functions of time and maximum curvature change extraction approach from daily NBAR-NDVI and NBAR-EVI. A Savitzky–Golay filter was used for noise reduction before the logistic curves were fitted to the

data. According to Zhang *et al.* [24], the logistic function is defined as

$$y(t) = \frac{c}{1 + e^{a+bt}} + d$$

where  $t$  is time in DOY,  $y(t)$  is the VI value at time  $t$ ,  $a$  and  $b$  are fitting parameters,  $c + d$  is the maximum VI value, and  $d$  is the initial background VI value. Greenup onset dates were estimated as the time when the fitted logistic curve experienced the greatest curvature change during the spring season time window [24]. This technique is currently used for producing MODIS global LSP products [48].

### C. Data Fusion of Landsat and MODIS

Landsat 30-m data provide spatial details that are good for monitoring land surface variations for local scale patches of  $\sim 1$  ha. However, the 16-day revisit cycle, along with cloud frequencies, has limited its use for studying seasonal processes, which rapidly evolve during the year. In cloudy areas, Landsat acquisition is limited to only a few clear images per year at best, which is insufficient for extracting reliable phenology metrics. On the other hand, MODIS sensors aboard the NASA Earth Observing System (EOS) Terra and Aqua satellites provide daily global observations that are valuable for capturing rapid surface changes and phenology, but with coarse spatial resolutions (250 m to 1 km). To combine the finer spatial resolution (30 m) of Landsat with the daily temporal frequency of MODIS, Gao *et al.* [41] developed the STARFM. This model is able to generate valuable information for applications that require high resolution in both time and space [43]. Such data fusion process may be understood as using daily MODIS information to make a “time correction” to infrequent Landsat data. The predicted images can capture rapid seasonal changes from MODIS data while retaining the Landsat spatial details.

Several new approaches have been recently developed to improve the initial STARFM for prediction in complex heterogeneous areas [49] or areas with rapidly changing land covers [50]. In this paper, we used the original STARFM approach to fuse Landsat and MODIS given its flexibility in using a single Landsat and MODIS pair. The recently developed approaches such as the Enhanced STARFM [49], the Spatial Temporal Adaptive Algorithm for mapping Reflectance Change [50], and the SParse-representation-based SpatioTemporal reflectance Fusion Model [51] require two input pairs of Landsat and MODIS images. The STARFM approach accepts one input pair in the prediction; therefore, it is suitable for our study area where high-quality cloud-free Landsat images were very limited due to weather influenced by frequent polar front passing and moisture from the Great Lakes.

Fifteen Landsat 5 Thematic Mapper (TM) and 15 Landsat 7 Enhanced TM Plus (ETM+) images (WRS-2 path 25 and row 28) from 2006 to 2009 were acquired and used in this study. All Landsat data were calibrated and atmospherically corrected to surface reflectance using Landsat Ecosystem Disturbance Adaptive Processing System (LEDAPS) [52] downloaded from the NASA LEDAPS website (recent version now available from <https://code.google.com/p/ledaps/>). Among the 30 available

TABLE II  
LIST OF HIGH-QUALITY AND CLEAR LANDSAT IMAGES (WRS-2 PATH 25 AND ROW 28) USED TO PAIR WITH MODIS NBAR DATA FOR DATA FUSION IN THE STUDY AREAS FROM 2006 TO 2009. DATE IS IN DOY

Landsat Instrument	Acquisition Date	Date (DOY)	Prediction Period (DOY)
L5 TM	April 8, 2006	98	<100
L5 TM	April 27, 2007	117	100-139
L5 TM	August 17, 2007	229	140-259
L5 TM	October 4, 2007	277	260-299
L5 TM	November 10, 2009	314	>=300

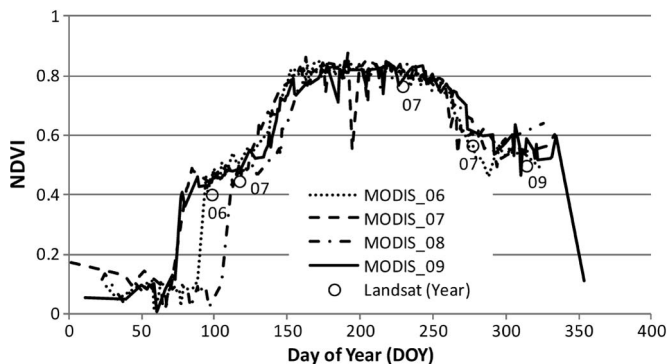


Fig. 3. MODIS NBAR NDVI from 2006 to 2009 in the study area overlaid with Landsat 5 TM observations that were used to pair with the MODIS data for fusion (cf. Table II).

Landsat images, most of them were partially covered by either cloud or snow or had data gaps. Only five Landsat 5 TM images (see Table II) were clear over the entire multiyear observation period (2006–2009) and selected to pair with the MODIS daily surface reflectance acquired from the same dates for Landsat–MODIS data fusion processing. Since Landsat 5 and Terra/Aqua MODIS have different orbital parameters, daily observations from the two sensors have different viewing and solar geometries. The use of daily MODIS NBAR products [35], [37] was therefore necessary to make sure that both MODIS and Landsat data have similar view angles (close to nadir) for a more consistent fusion process. As Landsat 7 images have had data gaps due to the failure of the Scan Line Corrector (SLC) in ETM+ instrument since May 2003, they were excluded from building Landsat and MODIS data pair for the data fusion processing; otherwise, all the data gaps would be carried over to the fused products. However, 15 ETM+ scenes and additional 10 TM scenes that were not used for fusion were all used to compose the Landsat time series for extracting phenological metrics. This approach was needed to retain all information contained in the available Landsat scenes. Data gaps in ETM+ images were labeled as missing values in constructing the time-series function.

Specifically, Fig. 3 shows the annual NDVI curves from MODIS and points from TM averaged from a subset area around the study area ( $1000 \times 1000$  Landsat pixels). The five clear Landsat TM images (cf. Table II) were used to build MODIS–Landsat image pairs to cover different segments of an NDVI annual curve. They were used to generate the synthesized Landsat data for the entire period of 2006–2009. Ideally, the selection of Landsat and MODIS data pair should be close to the prediction (MODIS) date. However, as there were not

enough clear Landsat scenes available in each year to bracket the prediction period, only one input pair was used to predict Landsat surface reflectance for each specific annual time period across 2006–2009. For example, we used MODIS–Landsat image pair on April 27, 2007 (DOY = 117) and MODIS daily nadir-view surface reflectance to produce the 30-m fused images for the early season (DOY between 100 and 139) of each year from 2006 to 2009. This single-pair-based fusion process as limited by available data is acceptable given that there were no large land cover conversions from 2006 to 2009 in our study areas and the spatial variations of land cover from year to year remained relatively consistent. The single pair option for STARFM was also explored and found effective in mapping daily surface reflectance [53] and daily evapotranspiration [54] when clear Landsat observations were limited or the changes of surface conditions were abrupt. Previous studies further revealed that STARFM works well when major land surface variations are from phenology/seasonal change alone [41], [43], [49]. Finally, the fused Landsat surface reflectances were combined with all available original Landsat TM and ETM+ surface reflectances (with SLC-off scenes included) from each year. Temporally optimized NDVI and EVI time series at Landsat spatial resolution for each year were in turn computed and used to characterize LSP at the community level. For greenup onset date extraction, the same logistic model approach [24] was used for fused Landsat time series during the late winter to summer time period of each year.

#### D. Comparing Ground and Satellite Observations

The north and south study areas, respectively, overlapped with five and six 500-m MODIS NBAR image pixels (see Fig. 1). A weighted extraction method was used to derive MODIS NBAR VI values of the intersected fractions from the full pixels. The weights were ratios of averaged NDVI changes within the fraction and the entire corresponding MODIS pixel, respectively, as estimated from high-resolution QuickBird images. The QuickBird-based NDVI changes were used as ground reference and were not validated with *in situ* measurements. Area-weighted averaging was then used to calculate the VI values for each study area at different time points. For the smaller initial study area, VI values were extracted using the same approach. Extraction was done under native MODIS sinusoidal projection, given a Universal Transverse Mercator (UTM)-to-sinusoidal reprojection yields higher spatial accuracy [55]. The greenup onset estimates were then extracted from the MODIS NBAR VI time series for the respective study area polygons (north, south, and initial). Both the time series of VI and LP indices, as well as the greenup onset dates determined from ground and satellite measurements, were compared by study area/year. Deciduous and coniferous LP indices were compared with MODIS NBAR VI time series directly. The difference between greenup onset dates estimated from VI and deciduous LP index were quantified using the mean absolute error (MAE) statistics. The overall relative agreement between ground and satellite greenup measures was also evaluated with a Spearman's rank correlation analysis [56]. The Spearman's rank correlation coefficient (Spearman's rho) quantifies the

statistical dependence of two ranked variables and was therefore useful for assessing whether the ground and satellite measures matched each other in relative variations across years and study areas. Furthermore, the integrated LP index (designed to be comparable to VI in unit dimension [0–1]) time series were standardized according to the following formula:

$$LP_s = \frac{LP_{obs} - LP_{min}}{LP_{max} - LP_{min}}$$

where  $LP_s$  is the standardized value, and  $LP_{obs}$ ,  $LP_{max}$ , and  $LP_{min}$  are the observed, maximum, and minimum values, respectively. The VI time series were standardized using the same formula and cross compared with standardized LP for only observations available on the same dates. The root-mean-square errors (RMSEs) between the integrated LP and the respective VI (EVI and NDVI) time series were calculated accordingly. In addition, regression slopes for EVI and NDVI were compared using analysis of covariance (ANCOVA) [56] to check whether the relationships between the integrated LP and the two VI types respectively were significantly different.

We further compared the MODIS–Landsat fused LSP with LP at the community level. The distribution of generalized communities for both north and south study areas is presented in Fig. 1. Landsat resolution (30 m) data were first resampled to 5 m (using the nearest neighbor assignment) in consideration of small-sized plant communities (e.g., grass/shrub land opening) and for a finer partitioning of pixel values at the community boundaries. For both VI and greenup onset date estimates, spatial averages of pixels contained within respective communities were calculated from the resampled data. For all communities, MAE was calculated between the greenup onset dates of fused LSP and deciduous LP by year, study area, and VI type. MAE was also computed for individual community for all observation years and both VI types, respectively. Assuming the area of a community has potential influence on the accuracy of LSP detection, we also looked at the correspondence between MAE and community size. The Spearman’s rank correlation analysis was used to check the agreement of the variations of LSP greenup onset and deciduous LP full bud burst across communities. Finally, we directly compared the fused VI and the integrated LP index time series for all communities using VI and LP values acquired on the same dates. Similar to the study-area-level analysis, standardization, RMSE, and ANCOVA were used to check the levels of agreement between VI and LP time series at the community level in terms of timing for the targeted spring phenology process.

### III. RESULTS

At the study area level, spring greenup onset dates extracted from daily MODIS NBAR VI time series predicted deciduous LP full bud burst dates with fairly low errors (see Table III). Given the initial study area (625 m × 275 m) was smaller compared to the 500-m MODIS pixel size, the comparison was separately made for the initial study area (2006–2007) and the two expanded and larger (625 m × 625 m) study areas (2008–2009). The LSP greenup onset dates for the larger study areas across the two years had an overall MAE (for both

TABLE III  
GREENUP ONSET DATES (DOY) FOR EACH STUDY AREA/YEAR ACCORDING TO STANDARD 16-DAY MODIS (FOR 2008 AND 2009 ONLY) [19] AND DAILY MODIS NBAR AND FULL BUD BURST (FBB) DATES (DOY) OF GROUND-BASED LP (FOR DECIDUOUS [DECI] AND CONIFEROUS [CONI] TREES, RESPECTIVELY). LP ESTIMATES WERE BASED ON UPSCALED MEASUREMENTS FOR A STUDY AREA. GREENUP ONSET DATES WERE ACCORDING TO MODIS PIXEL-LEVEL PREDICTIONS EXTRACTED FROM EACH STUDY AREA. THE MAES (IN DAYS) WERE CALCULATED BETWEEN CORRESPONDING LSP AND DECIDUOUS LP ESTIMATES (IN BOLD LETTER)

		Standard MODIS LSP		MAE	MODIS NBAR LSP		MAE	Ground LP	
		NDVI	EVI		NDVI	EVI		FBB <sub>deci</sub>	FBB <sub>coni</sub>
2006	Initial	-	-		134	123	7.48	<b>121</b>	131
2007	Initial	-	-		128	119	4.37	<b>127</b>	134
MAE					6.66	2.18	5.92*		
2008	North	139	138	0.5	147	142	6.56	<b>138</b>	146
	South	141	136	2.5	141	140	3.72	<b>137</b>	146
2009	North	122	133	7.5	138	132	3.48	<b>135</b>	142
	South	116	132	8	129	125	4.17	<b>131</b>	143
MAE		8.25	1	4.63	4.67	4.29	4.48*		

\* indicates the overall MAE derived from averaging MAE across respective years and study areas.

NDVI and EVI) of 4.48 days, slightly smaller than that of the previous study using the standard VI product (4.63 days). With the use of daily NBAR data, the MAE for the NDVI-based estimate notably improved from 8.25 to 4.67 days, but the MAE for EVI turned out to be larger (4.29 days versus 1 day in our previous study). For the north and south study areas across 2008 and 2009, respectively, similar to results from our previous study, daily MODIS NBAR greenup onset dates fully captured the spatial and temporal differences of LP full bud burst dates—both showing that phenology in 2009 was earlier than that in 2008 and that phenology in the south study area was more advanced than that in the north study area.

The daily NBAR VI-based greenup onset for the initial study area had larger errors (overall MAE of 5.92 days) than that for the complete study areas. In addition, the detected interannual variation did not agree with that of the ground LP from 2006 to 2007. Nonetheless, relatively significant Spearman’s ranked correlations (see Table IV) indicated that daily MODIS NBAR VI-based greenup dates captured the overall spatiotemporal variations across the four years at the study area level in spite of the discrepancies (mainly from the initial study area). Additionally, the specific MAE for EVI (2.18 and 4.29 days) was consistently smaller than that for NDVI (6.66 and 4.67 days) for the initial and complete study areas, respectively.

Moreover, comparison of the time series of VI and deciduous and coniferous LP indices demonstrated the systematic difference between ground and satellite observations—landscape phenological trajectory advanced faster than the LSP change (see Fig. 4). However, the onset of fast VI increase largely occurred near the time when deciduous LP reached the full bud burst level (400), which was also in accordance to the close match with greenup onset date estimates (cf. Table III). When the integrated LP was compared with VI values, linear correspondence yielded coefficients of determination values of 0.49 and 0.39 for NBAR-EVI and NBAR-NDVI, respectively, and RMSE up to a quarter (0.23–0.26) of the data range (see Fig. 5). ANCOVA results did not show significant differences between the slopes of EVI and NDVI regression lines, which were both close to and below 1. NBAR-EVI showed a slightly



TABLE IV  
 SPEARMAN'S RANK CORRELATION COEFFICIENTS BETWEEN GREENUP ONSET DATES BY STUDY AREA/YEAR ACCORDING TO STUDY-AREA-LEVEL DAILY MODIS NBAR AND COMMUNITY-LEVEL FUSED LANDSAT-BASED LSP AND CORRESPONDING GROUND-BASED DECIDUOUS FULL BUD BURST LP. THREE STUDY-AREA-LEVEL ESTIMATES AND 11–17 COMMUNITY LEVEL ESTIMATES ACROSS FOUR YEARS PARTICIPATED THE RANK CORRELATION ANALYSIS. STATISTICALLY SIGNIFICANT VALUES ARE INDICATED WITH \* ( $\alpha < 0.05$ ) AND • ( $\alpha < 0.10$ )

	MODIS NBAR LSP		Fused Landsat LSP									
	2006-2009		2006-2009		2006		2007		2008		2009	
	NDVI	EVI	NDVI	EVI	NDVI	EVI	NDVI	EVI	NDVI	EVI	NDVI	EVI
Spearman rho	0.83•	0.90*	0.23•	0.79*	0.45	-0.22	-0.38	-0.15	0.01	0.12	0.08	0.30

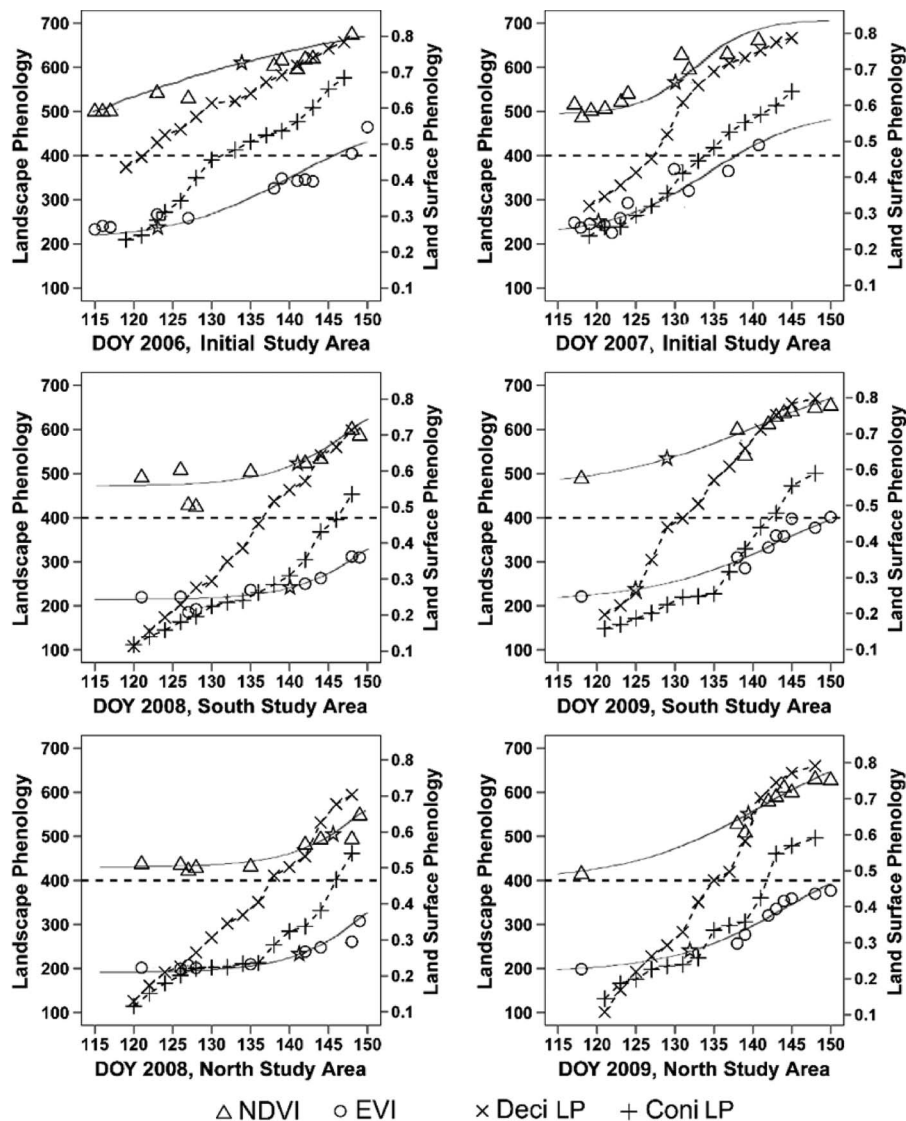


Fig. 4. Side-by-side comparison of specific LP indices (deciduous—Deci; coniferous—Coni) with daily MODIS NBAR EVI and NDVI time series. The *x*-axis DOY indicates day of year. The left *y*-axis is according to the field protocol of spring phenology; the right *y*-axis indicates VI ratios. All available actual observations were included except that one obvious outlier (possibly due to the shadow effect) in the 2007 NDVI time series was removed. The segments of logistic curves (fitted for VI data from DOY81 to 230) are provided. The full bud break reference line (400) and the location of predicted greenup onset (with a star) on VI curves are provided in each figure (cf. Table III).

closer match with the integrated LP index than NBAR-NDVI, as indicated by larger  $R^2$  and smaller RMSE values.

At the community level, greenup onset estimates from fused Landsat data also agreed with deciduous LP full bud burst dates with relatively small errors (see Table V and Fig. 6). Across the communities, the overall MAE was 7.16 days for the initial

smaller study area and 4.11 days for the eventual expanded study areas. The two largest communities (maple- and pine-dominated forests) in the north study area appeared to have the least MAE (less than two days). However, the third largest but less distinct community (mixed aspen/fir forest, largest in the initial study area) had relatively large errors (six to nine days).

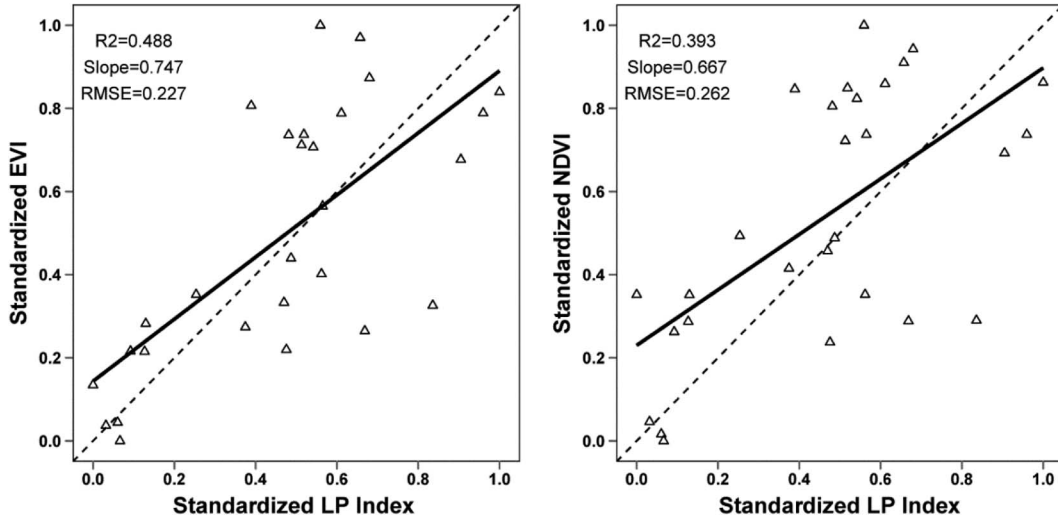


Fig. 5. Study-area-level comparison of the integrated LP index and daily MODIS NBAR VIs (EVI and NDVI). Only observed ground and satellite data on the same dates (for all four years 2006–2009) were included. Standardization  $([observation - minimum]/[maximum - minimum])$  was applied to both LP and VI data, and a 1 : 1 line is provided for each comparison. The ANCOVA result for the regression lines showed a  $p$ -value of 0.72, suggesting that the two slopes are not significantly different from one another.

TABLE V  
GREENUP ONSET DATES (DOY) FOR EACH COMMUNITY/YEAR ACCORDING TO THE FUSED LANDSAT ESTIMATES. THE MAES (IN DAYS) OF LSP ESTIMATES FROM THE DECIDUOUS LP ESTIMATES (FULL BUD BURST-FBB\_deci) ARE PROVIDED. EACH COMMUNITY HAS A SINGLE ESTIMATE FROM GROUND-BASED AND UPSCALED LP AND SATELLITE-BASED LSP, RESPECTIVELY. AREAS OF COMMUNITIES ARE ALSO PROVIDED

Communities	Ground LP		Fused Landsat LSP				MAE	Area (ha)
	2006	2007	2006		2007			
	FBB_deci	FBB_deci	NDVI	EVI	NDVI	EVI		
Alder bush (Initial)	122	123	134	131	123	119	6.49	0.19
Aspen/fir woods (Initial)	119	128	132	128	122	118	9.46	7.72
Grass/shrub land (Initial)	122	125	132	132	119	125	6.60	0.06
Hardwood stand (Initial)	122	127	128	130	118	118	8.18	0.25
Highly mixed area (Initial)	124	127	134	128	122	118	7.09	0.78
Old-growth residue (Initial)	122	126	131	125	122	116	6.66	0.76
Pine woods (Initial)	122	127	129	127	120	117	6.94	0.91
Sparse aspen/fir woods (Initial)	121	127	130	129	119	119	8.20	2.57
Sphagnum bog (Initial)	123	125	132	125	124	114	5.91	1.81
Forested wetland1 (Initial)	122	126	130	130	119	122	6.71	0.99
Forested wetland2 (Initial)	128	128	134	128	118	119	6.47	1.09
MAE			9.12	6.04	5.78	7.68	7.16*	
	2008	2009	2008		2009			
	FBB_deci	FBB_deci	NDVI	EVI	NDVI	EVI		
Alder bush (South)	136	132	133	140	136	131	2.89	0.73
Aspen/fir woods (South)	136	128	127	140	136	130	5.80	12.15
Grass/shrub land (South)	137	133	129	140	134	131	3.34	0.63
Hardwood stand (South)	137	133	132	141	135	133	2.60	1.85
Highly mixed area (South)	138	134	130	141	136	130	4.24	5.82
Old-growth residue (South)	137	133	129	142	137	130	5.02	0.76
Pine woods (South)	137	134	130	144	136	134	4.03	4.84
Sparse aspen/fir woods (South)	136	129	130	140	135	131	4.39	6.54
Sphagnum bog (South)	137	134	129	143	137	130	5.20	1.81
Forested wetland1 (South)	137	132	124	138	134	131	4.25	2.28
Forested wetland2 (South)	140	135	123	141	136	131	5.72	1.09
Tamarack wetland (North)	138	135	123	141	138	128	6.91	1.72
Grass/ shrub land (North)	138	137	136	135	134	132	3.17	1.70
Maple woods (North)	138	135	136	139	134	133	1.40	20.56
Highly mixed area (North)	138	132	129	141	135	128	4.54	1.69
Pine woods (North)	138	135	138	142	136	133	1.78	13.15
Pure aspen stand (North)	138	131	129	142	136	130	4.63	0.10
MAE			7.40	3.46	3.00	2.59	4.11*	

\* indicates the overall MAE derived from averaging MAE across all communities and years.

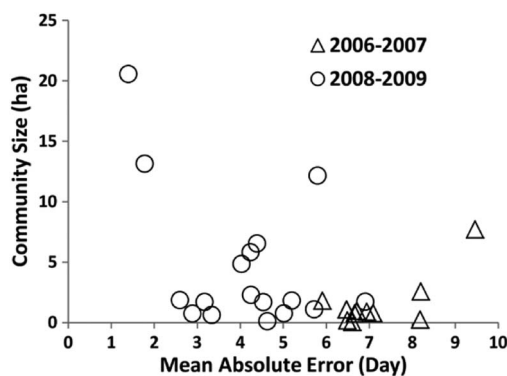


Fig. 6. MAEs of Landsat fused community-level greenup onset date estimates from deciduous LP full bud burst dates, relative to the community size (cf. Table V). Estimates for the initial study area (2006–2007) and the complete study areas (2008–2009) are separately shown with different symbols.

EVI-based greenup onset estimates captured the interannual LP difference between 2008 and 2009 consistently for all the communities. However, interannual variations of NDVI-based estimates for 2008 and 2009, as well as greenup onset dates for the initial study area in 2006 and 2007, did not show a temporal agreement for most communities. In addition, the Spearman's rank correlations (see Table IV) reflected a better agreement of EVI-based greenup onset estimates at the community level over time and space. However, LSP did not seem to capture the spatial variations of LP across communities, as indicated by the insignificant and inconsistent rank correlation coefficients for each individual year and all communities. Furthermore, direct comparisons of the integrated LP index with VI values at the community level (see Fig. 7) showed stronger linear agreements than those at the study area level—coefficients of determination values were 0.72 and 0.62 for EVI and NDVI, respectively. NBAR-EVI also showed higher  $R^2$  and smaller RMSE than NBAR-NDVI relative to the integrated LP at the community level.

#### IV. DISCUSSION

With the daily MODIS NBAR VI data, LSP estimation of greenup onset dates at the study area level agreed with deciduous LP full bud burst dates in a more consistent manner between NDVI and EVI. Particularly in comparison with the previous study utilizing 16-day standard MODIS VI products [19], the overall MAE for NDVI was reduced from eight days to less than five days. The agreement for EVI-based LSP did not show improvement (the earlier estimate had only one day of the overall MAE), but it is likely that the less than five days of MAE for greenup onset estimates represents a more realistic error level that LSP can achieve, given the large departures between EVI and NDVI estimates shown in the earlier study. Daily NBAR MODIS-based greenup onset date estimation demonstrated a slight advantage of using EVI over NDVI. In addition, EVI did better capture the spatial and temporal variations, as indicated by the greater rank correlation for greenup onset date estimates, and had a closer match with the integrated LP when time series were compared.

The daily NBAR VI provides consistent nadir views and daily frequency needed to track phenology and reduces the variability due to view angle change and uncertainty from large data gaps. In our study, the use of daily NBAR MODIS VI versus standard product has shown improvement on greenup onset detection for NDVI only, perhaps due to the already very close estimates for EVI in our previous study. However, these technical improvements did seem to provide higher stability in keeping the errors of both NDVI and EVI estimates low. The NBAR MODIS VI was shown to be better in comparison to the standard VI for LSP monitoring [25], [57]. This study further utilized daily NBAR data to increase the available temporal resolution. However, given that the BRDF retrieval uses all cloud-free data available, it is difficult to evaluate the respective contributions of view angle correction (NBAR) and daily retrieval frequency to improve LSP monitoring as both aspects are important. In addition, we utilized only cloud-free data without gap interpolation; therefore, the temporal resolution improvement was still limited by weather conditions. Furthermore, MODIS NBAR can be based on Terra-only (MOD43), Aqua-only (MYD43), and mixed (MCD43), and the results showed that although our high-quality pixels were equivalent values from Terra as from Aqua, many more high-quality pixels were available when data from both MODIS instruments were combined. From the perspective of maintaining long-term LSP monitoring with MODIS NBAR, we are aware that when one instrument fails, there will be fewer high-quality pixels for each BRDF retrieval, but the available high-quality pixel values from the remaining sensor will still provide consistent results.

The discrepancy with the comparisons using the initial two years (2006 and 2007) of observation is likely related to the spatial mismatch of ground–satellite data—the initial study area overlapped with very small fractions of five different MODIS pixels (see Fig. 1). Possible uncertainties with matching MODIS pixels to relatively small study areas could also arise from the MODIS gridding artifacts, which allowed spatial shifts of observations to fit recorded signals into the predefined grids [58]. The initial study area was about half the size of a complete study area because our intended transecting work was incomplete in 2006 and 2007 due to limited resources and harsh field conditions in the initial field campaign in 2005. The relatively larger error range for the smaller initial study area greenup onset date detection in comparison to the complete study areas is also shown in the community-level estimates, as indicated in Fig. 6. The coherent spatiotemporal agreement of LSP with LP greenup onset for the two complete study areas further suggested that ground validation is better conducted with observations representing areas large enough to be comparable with the spatial resolution of satellite data [59]. Our transects, however, did not match a complete nominal MODIS pixel. We were aware of this limitation but did not pursue this given the uncertainty of the true location of a MODIS pixel due to its inherent geolocation error ( $\pm 50$  m). Therefore, additional errors may exist with extracting values from multiple pixels overlapped with the study areas. Had similar work been engaged in the future, it is recommended to preselect sampling grids that match targeted satellite pixels as close as possible.

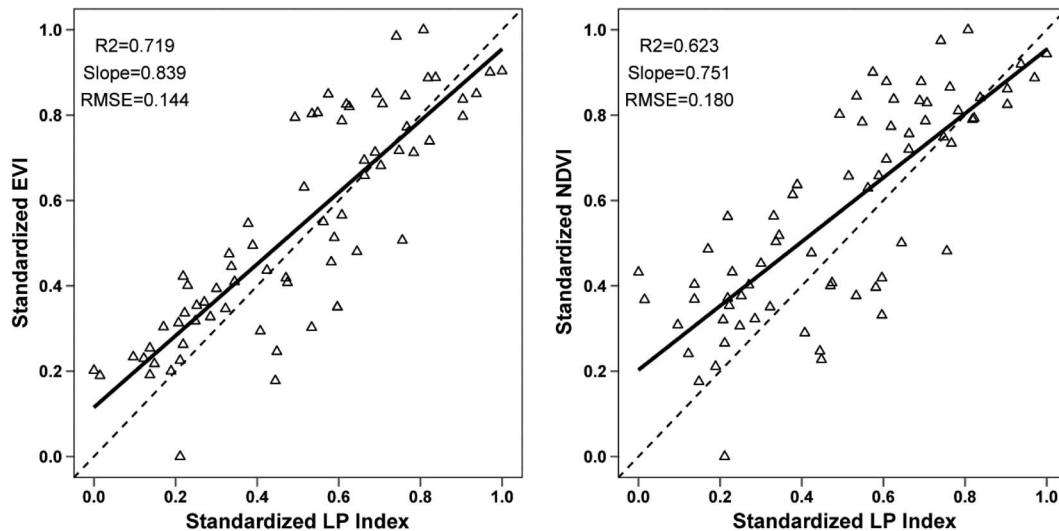


Fig. 7. Community-level comparison of the integrated LP index and MODIS-Landsat fused VIs (EVI and NDVI). Only actually observed ground and satellite data that matched in dates (for all four years 2006–2009) were included. Standardization ( $[\text{observation} - \text{minimum}] / [\text{maximum} - \text{minimum}]$ ) was applied to both LP and VI data, and a 1 : 1 line is provided for each comparison. The ANCOVA result for the regression lines showed a  $p$ -value of 0.35, suggesting that the two slopes are not significantly different from one another.

In addition, the change rate disagreement between the LSP and LP trajectories indicated that the post-bud burst phenology contributes the most to the land surface phenological change; and the early phenological stages related to bud development do not noticeably affect the satellite signals. This finding was also noted in our previous study that compared interpolated time series from the 16-day MODIS VI [19]. The current study was based on actual observation points from the daily MODIS NBAR data. The consistently smaller than 1 regression slope lines for direct VI and integrated LP index comparison at both the study area and community levels implied the same relationship. The results confirmed that the systematic difference in time series was due to our field protocol including phenological processes that are either undetected (e.g., bud swollen) by or apparent (e.g., leaf unfolding) to remote optical sensors.

Comparisons at the community level based on daily MODIS-Landsat fused estimates yielded a similar error range as of the study-area-level analysis. However, given the significantly improved spatial resolution, four days of the overall MAE (for communities across the larger study areas) suggested a prediction with good confidence. It would be more encouraging if Landsat resolution LSP could have picked up the differences among the different communities, but such information was likely lost because of the error range exceeding the subtle intercommunity variations within the study areas. The mixed forest investigated in this study is relatively heterogeneous in community composition, but the forest is fairly continuous in canopy coverage, and the expressed magnitude of phenological difference may not be large enough to show in Landsat images. We speculate that in more heterogeneous vegetated landscapes with plant communities that have larger spectral reflectance differences, the fused product may be more useful for providing information of finer spatial variability in phenology. In addition, the prediction seemed to be more accurate for larger and more uniform communities, implying that the composition and

size of vegetation cover can affect the quality of information extracted from fused LSP. On the other hand, the accuracy of fused LSP may be affected by the limited availability of clear-scene Landsat-MODIS pairs, which may contribute to the overall uncertainties of community-level phenology estimates.

Recently, the LEDAPS surface reflectance product has been quality checked by the U.S. Geological Survey (USGS) Earth Resources Observation and Science (EROS) Center [60]. The USGS EROS has released the Landsat surface reflectance data record ([http://landsat.usgs.gov/CDR\\_LSR.php](http://landsat.usgs.gov/CDR_LSR.php)), which can be directly used in later data fusion processing. In our study, all cloud-free Landsat data were used to generate fused LSP product. Partially cloud-contaminated Landsat scenes may be more useful if an accurate cloud mask is available. Several cloud mask algorithms for Landsat imagery have been developed in past years [61]–[64]. However, operational use at the Landsat pixel level is still a challenge. A recently developed Fmask algorithm [64] has demonstrated the feasibility in detecting cloud and cloud shadows at a highly confident level, which could pave a way to producing cloud confidence bits in the data quality band for Landsat 8 [65].

In our initiative to cross validate LSP for two nearby study areas, we undertook an intensive field observation approach to overcome the scale mismatch between satellite and ground observations. We attempted to optimize the spatial density, temporal frequency, and areal coverage of field phenological sampling to make it more comparable to the satellite data products. In addition, downscaling of coarse-resolution LSP through fusing MODIS with Landsat data provides another perspective to link satellite measures with ground observations, akin to the multiyear Landsat aggregation attempt in [29]. Thus, the innovations in both ground data collection and satellite data processing enabled the current study comparing spatiotemporally enhanced LSP and LP, collectively allowing analyses at both the community and study area scales. Furthermore, the deciduous and coniferous specific LP indices as developed through

combining plant phenology and landscape heterogeneity allowed direct comparison of physiologically meaningful plant phenophases with land surface reflectance change. However, high-resolution multitemporal QuickBird images were used as ground truth in our upscaling approach for separating the effect of deciduous and coniferous trees. This may have introduced biases to, particularly, the reflectance-calibrated and integrated LP index. We speculate that the upscaling of conventional observer-based phenology data may be improved with ground observations of similar nature as optical remote sensing, such as approaches using spectroradiometers or networked digital cameras [66]–[68].

The limited geographic coverage of intensively collected field data remains a challenge to gauge the representativeness of our validation results for broader regions. Given that our field data covered only a small sample of the temperate mixed forest in the U.S., similar work done in other temperate forests would help in assessing the applicability of the results from this study. The major hindrance of acquiring such high-density data is the intensive field labor required. However, a more cost-effective approach may be adopted with reduced temporal observation frequency [32] and perhaps a combined use of spectroradiometers/digital cameras. Therefore, it may be possible to extend the cross-comparison work from temperate forest to other biomes and vegetation types, including agricultural lands. Such usage will certainly require more testing and validation of phenological products for these additional vegetation types. Additionally, the application of fused LSP needs to be further explored in study areas with diverse amounts of landscape heterogeneity, various conditions, and vegetation cover types to potentially enable more detailed monitoring of vegetation changes caused by processes such as climate change and/or natural/human disturbances.

While progress was made in this study toward phenological product validation, future LSP validation still faces a number of challenges. First, the validation target time period needs to be extended from spring to autumn, particularly for temperate biomes, therefore covering phenological transitions marking the start and the end of growing season. The ability of current LSP approaches may be different for greenup than brown-down. Such efforts will improve the accuracy of LSP as inputs to biogeochemical and climatic models [69]. Second, evaluations of different LSP products from sensors other than AVHRR and MODIS, such as SPOT-Vegetation and Medium Resolution Imaging Spectrometer (MERIS), and now Visible Infrared Imaging Radiometer Suite (VIIRS) and indices other than NDVI and EVI [10], [59], such as MERIS Terrestrial Chlorophyll Index [70], Leaf Area Index [71], and fraction of Photosynthetically Active Radiation [72], will be useful for guiding specific applications in choosing appropriate data sources. Furthermore, it remains a challenge to reconcile different processing algorithms that could be applied to VI time series for extracting LSP metrics [73]. For a given sensor-specific data stream, the spatial variations in patterns across LSP products are likely to be relatively consistent for continental- to global-scale pattern detection, but temporal differences among LSP products will be manifested as uncertainties for applications at local and regional scales.

TABLE VI  
ACRONYMS AND CORRESPONDING TERMS (ONLY THOSE REPEATED MULTIPLE TIMES ARE LISTED, ACCORDING TO THE ORDER OF THEIR FIRST APPEARANCE IN THE TEXT)

Acronyms	Terms
LSP	Land Surface Phenology
LP	Landscape Phenology
MODIS	Moderate Resolution Imaging Spectroradiometer
BRDF	Bidirectional Reflectance Distribution Function
NBAR	Nadir BRDF-Adjusted Reflectance
VI	Vegetation Index
NDVI	Normalized Difference Vegetation Index
EVI	Enhanced Vegetation Index
AVHRR	Advanced Very High Resolution Radiometer
MVC	Maximum Value Composite
STARFM	Spatial and Temporal Adaptive Reflectance Fusion Model
DOY	Day of Year
TM	Thematic Mapper
LEDAPS	Landsat Ecosystem Disturbance Adaptive Processing System
ETM+	Enhanced Thematic Mapper Plus
SLC	Scan Line Corrector
MAE	Mean Absolute Error
RMSE	Root Mean Square Error
ANCOVA	Analysis of Covariance
Suomi NPP	Suomi National Polar-orbiting Partnership
VIIRS	Visible Infrared Imaging Radiometer Suite

## V. CONCLUSION

The results from this study suggest that springtime LSP derived from spatiotemporally enhanced VI data can improve our ability to detect more detailed LP information. Compared to 16-day composited VIs, daily MODIS NBAR VI time series for LSP derivation appeared to support more consistent estimation of phenological transition dates across the two indices (EVI and NDVI) with less than five days of MAE. For the study areas investigated, daily MODIS NBAR data appeared more reliable for LSP monitoring of rapidly changing seasonal vegetation dynamics at coarse spatial scales. Daily MODIS NBAR data also confirmed that post-bud burst phenology of deciduous trees contributes the most to VI change. The daily NBAR MODIS–Landsat fused LSP captured the greenup onset dates of community-level phenology with the overall MAE of about four days, with generally smaller errors for larger and more uniformed communities. In addition, the fused VI time series showed a closer match (lower MAE) with the integrated LP at the community level than that of the study-area-level comparison from using only MODIS data. However, the community-level LSP was not able to track small differences among different forest communities in our study areas. The limited number of cloud free MODIS and Landsat data available to our study site may have influenced the overall accuracy of fused LSP estimates. Nevertheless, the temporally and spatially enhanced remote sensing data were shown to be useful in our limited test for enabling more detailed phenological monitoring. With data from the newest generation of Earth resource observation efforts such as the Landsat 8 Operational Land Imager and the Suomi National Polar-orbiting Partnership (Suomi NPP) VIIRS, we are hopeful that satellite-based phenological monitoring with enhanced spatial and temporal resolutions will become increasingly useful for phenological applications requiring details that are currently beyond the reach of time composited VI or a single type of remote sensor.

## ACKNOWLEDGMENT

The authors would like to thank J. Hanes, R. Dearing, A. Fusco, J. Hatzis, J. Hurry, P. O'Kane, I. Park, and V. Seamster, who all contributed to this project as phenological observers; A. Halfen and J. Hanes for helping build transects in the expanded study areas; the entire staff at the Kemp Natural Resources Station for their support during all of the field campaigns; J. Phillips for reviewing the entire manuscript and providing helpful comments; and two anonymous reviewers for their constructive comments. The authors also appreciate insights from participants of the 2012 Land Surface Phenology Product Validation Meeting of the CEOS WGCV Land Product Validation Subgroup. Any use of trade, firm, or product names is for descriptive purposes only and does not imply endorsement by the U.S. Government. USDA, NASA, and USGS are equal opportunity providers and employers.

## REFERENCES

- [1] M. D. Schwartz, *Phenology: An Integrative Environmental Science*. Dordrecht, The Netherlands: Kluwer, 2003.
- [2] J. T. Morisette, A. D. Richardson, A. K. Knapp, J. I. Fisher, E. A. Graham, J. Abatzoglou, B. E. Wilson, D. D. Breshears, G. M. Henebry, J. M. Hanes, and L. Liang, "Tracking the rhythm of the seasons in the face of global change: Phenological research in the 21st century," *Frontiers Ecology Environ.*, vol. 7, no. 5, pp. 253–260, Jul. 1, 2009.
- [3] X. Zhang, J. C. F. Hodges, C. B. Schaaf, M. A. Friedl, A. H. Strahler, and F. Gao, "Global vegetation phenology from AVHRR and MODIS data," in *Proc. IEEE Int. Geosci. Remote Sens. Symp.*, 2001, vol. 5, pp. 2262–2264.
- [4] K. M. de Beurs and G. M. Henebry, "Land surface phenology, climatic variation, and institutional change: Analyzing agricultural land cover change in Kazakhstan," *Remote Sens. Environ.*, vol. 89, no. 4, pp. 497–509, Feb. 2004.
- [5] E. Ivits, M. Cherlet, G. Tóth, S. Sommer, W. Mehl, J. Vogt, and F. Micala, "Combining satellite derived phenology with climate data for climate change impact assessment," *Global Planetary Change*, vol. 88/89, pp. 85–97, May 2012.
- [6] F. Tao, M. Yokozawa, M. Yokozawa, Y. Hayashi, and Y. Ishigooka, "Land surface phenology dynamics and climate variations in the North East China Transect (NECT), 1982–2000," *Int. J. Remote Sens.*, vol. 29, no. 19, pp. 5461–5478, 2008.
- [7] W. W. Hargrove, J. P. Spruce, G. E. Gasser, and F. M. Hoffman, "Toward a national early warning system for forest disturbances using remotely sensed canopy phenology," *Photogramm. Eng. Remote Sens.*, vol. 75, pp. 1150–1156, 2009.
- [8] J. P. Spruce, S. Sader, R. E. Ryan, J. Smoot, P. Kuper, K. Ross, D. Prados, J. Russell, G. Gasser, R. McKellip, and W. Hargrove, "Assessment of MODIS NDVI time series data products for detecting forest defoliation by gypsy moth outbreaks," *Remote Sens. Environ.*, vol. 115, no. 2, pp. 427–437, Feb. 2011.
- [9] M. E. Brown and K. M. de Beurs, "Evaluation of multi-sensor semi-arid crop season parameters based on NDVI and rainfall," *Remote Sens. Environ.*, vol. 112, no. 5, pp. 2261–2271, May 2008.
- [10] S. R. Garrity, G. Bohrer, K. D. Maurer, K. L. Mueller, C. S. Vogel, and P. S. Curtis, "A comparison of multiple phenology data sources for estimating seasonal transitions in deciduous forest carbon exchange," *Agric. Forest Meteorol.*, vol. 151, no. 12, pp. 1741–1752, 2011.
- [11] A. D. Richardson, R. S. Anderson, M. A. Arain, A. G. Barr, G. Bohrer, G. Chen, J. M. Chen, P. Ciais, K. J. Davis, A. R. Desai, M. C. Dietze, D. Dragoni, S. R. Garrity, C. M. Gough, R. Grant, D. Y. Hollinger, H. A. Margolis, H. McCaughey, M. Migliavacca, R. K. Monson, J. W. Munger, B. Poulter, B. M. Raczka, D. M. Ricciuto, A. K. Sahoo, K. Schafer, H. Tian, R. Vargas, H. Verbeeck, J. Xiao, and Y. Xue, "Terrestrial biosphere models need better representation of vegetation phenology: Results from the North American Carbon Program Site Synthesis," *Global Change Biol.*, vol. 18, no. 2, pp. 566–584, Feb. 2012.
- [12] X. Zhang, M. Friedl, and C. Schaaf, "Sensitivity of vegetation phenology detection to the temporal resolution of satellite data," *Int. J. Remote Sens.*, vol. 30, no. 8, pp. 2061–2074, 2009.
- [13] M. A. Friedl et al., "MODIS Collection 5 global land cover: Algorithm refinements and characterization of new datasets," *Remote Sensing of Environment*, vol. 114, no. 1, pp. 168–182, Jan. 2010.
- [14] J. Campbell, *Introduction to Remote Sensing*. New York, NY, USA: The Guilford Press, 2006.
- [15] A. Kross, R. Fernandes, J. Seaquist, and E. Beaubien, "The effect of the temporal resolution of NDVI data on season onset dates and trends across Canadian broadleaf forests," *Remote Sens. Environ.*, vol. 115, no. 6, pp. 1564–1575, Jun. 2011.
- [16] M. D. Schwartz and B. C. Reed, "Surface phenology and satellite sensor-derived onset of greenness: An initial comparison," *International Journal of Remote Sensing*, vol. 20, no. 17, pp. 3451–3457, 1999.
- [17] J. Morisette, J. Privette, and C. Justice, "A framework for the validation of MODIS land products," *Remote Sens. Environ.*, vol. 83, no. 1/2, pp. 77–96, Nov. 2002.
- [18] M. D. Schwartz and J. Hanes, "Intercomparing multiple measures of the onset of spring in eastern North America," *Int. J. Climatol.*, vol. 30, no. 11, pp. 1614–1626, Sep. 2010.
- [19] L. Liang, M. D. Schwartz, and S. Fei, "Validating satellite phenology through intensive ground observation and landscape scaling in a mixed seasonal forest," *Remote Sens. Environ.*, vol. 115, no. 1, pp. 143–157, Jan. 2011.
- [20] S. N. Goward, C. J. Tucker, and D. G. Dye, "North American vegetation patterns observed with the NOAA-7 Advanced Very High Resolution Radiometer," *Vegetatio*, vol. 64, no. 1, pp. 3–14, Dec. 1985.
- [21] C. O. Justice, E. Vermote, J. R. G. Townshend, R. DeFries, D. P. Roy, D. K. Hall, V. V. Salomonson, J. L. Privette, G. Riggs, A. Strahler, W. Lucht, R. B. Myneni, Y. Knyazikhin, S. W. Running, R. R. Nemani, Z. Wan, A. R. Huete, W. Van Leeuwen, R. E. Wolfe, L. Giglio, J.-P. Muller, P. Lewis, and M. J. Barnsley, "The Moderate Resolution Imaging Spectroradiometer (MODIS): Land remote sensing for global change research," *IEEE Trans. Geosci. Remote Sens.*, vol. 36, no. 4, pp. 1228–1249, Jul. 1998.
- [22] A. Huete, K. Didan, T. Miura, E. P. Rodriguez, X. Gao, and L. G. Ferreira, "Overview of the radiometric and biophysical performance of the MODIS vegetation indices," *Remote Sens. Environ.*, vol. 83, no. 1/2, pp. 195–213, Nov. 2002.
- [23] B. C. Reed, J. F. Brown, D. VanderZee, Thomas R. Loveland, W. James, and O. Donald, "Measuring phenological variability from satellite imagery," *J. Vegetation Sci.*, vol. 5, no. 5, pp. 703–714, Nov. 1994.
- [24] X. Zhang, M. A. Friedl, C. B. Schaaf, A. H. Strahler, J. C. F. Hodges, F. Gao, B. C. Reed, and A. Huete, "Monitoring vegetation phenology using MODIS," *Remote Sens. Environ.*, vol. 84, no. 3, pp. 471–475, Mar. 2003.
- [25] X. Zhang, M. A. Friedl, and C. B. Schaaf, "Global vegetation phenology from Moderate Resolution Imaging Spectroradiometer (MODIS): Evaluation of global patterns and comparison with in situ measurements," *J. Geophys. Res.-Biogeosci.*, vol. 111, no. G4, p. G04017, Dec. 2006.
- [26] Y. Shuai, C. Schaaf, X. Y. Zhang, A. Strahler, D. Roy, J. Morisette, Z. S. Wang, J. Nightingale, J. Nickeson, A. D. Richardson, D. H. Xie, J. D. Wang, X. W. Li, K. Strabala, and J. E. Davies, "Daily MODIS 500 m reflectance anisotropy direct broadcast (DB) products for monitoring vegetation phenology dynamics," *Int. J. Remote Sens.*, vol. 34, no. 16, pp. 5997–6016, 2013.
- [27] W. Xiao, Z. Sun, Q. Wang, and Y. Yang, "Evaluating MODIS phenology product for rotating croplands through ground observations," *J. Appl. Remote Sens.*, vol. 7, no. 1, pp. 073562–073562, 2013.
- [28] M. D. Schwartz, J. L. Betancourt, and J. F. Weltzin, "From Caprio's lilacs to the USA National Phenology Network," *Frontiers Ecol. Environ.*, vol. 10, no. 6, pp. 324–327, Aug. 2012.
- [29] J. I. Fisher, J. F. Mustard, and M. A. Vadeboncoeur, "Green leaf phenology at Landsat resolution: Scaling from the field to the satellite," *Remote Sens. Environ.*, vol. 100, no. 2, pp. 265–279, Jan. 2006.
- [30] J. I. Fisher and J. F. Mustard, "Cross-scalar satellite phenology from ground, Landsat, and MODIS data," *Remote Sens. Environ.*, vol. 109, no. 3, pp. 261–273, Aug. 2007.
- [31] L. Liang and M. D. Schwartz, "Landscape phenology: An integrative approach to seasonal vegetation dynamics," *Landscape Ecol.*, vol. 24, no. 4, pp. 465–472, Apr. 2009.
- [32] M. D. Schwartz, J. M. Hanes, and L. Liang, "Comparing carbon flux and high-resolution spring phenological measurements in a northern mixed forest," *Agric. Forest Meteorol.*, vol. 169, pp. 136–147, Feb. 2013.
- [33] E. A. Graham, E. C. Riordan, E. M. Yuen, D. Estrin, and P. W. Rundel, "Public Internet-connected cameras used as a cross-continental ground-based plant phenology monitoring system," *Global Change Biol.*, vol. 16, no. 11, pp. 3014–3023, Nov. 2010.
- [34] K. Hufkens, M. Friedl, O. Sonnentag, B. H. Braswell, T. Milliman, and A. D. Richardson, "Linking near-surface and satellite remote sensing measurements of deciduous broadleaf forest phenology," *Remote Sens. Environ.*, vol. 117, pp. 307–321, 2012.
- [35] C. B. Schaaf, F. Gao, A. H. Strahler, W. Lucht, X. Li, T. Tsang, N. C. Strugnell, X. Zhang, Y. Jin, J.-P. Muller, P. Lewis, M. Barnsley, P. Hobson, M. Disney, G. Roberts, M. Dunderdale, C. Doll,

- R. P. d'Entremont, B. Hu, S. Liang, J. L. Privette, and D. Roy, "First operational BRDF, albedo nadir reflectance products from MODIS," *Remote Sens. Environ.*, vol. 83, no. 1/2, pp. 135–148, Nov. 2002.
- [36] C. B. Schaaf, J. Liu, F. Gao, and A. H. Strahler, "MODIS albedo and reflectance anisotropy products from Aqua and Terra," in *Land Remote Sensing and Global Environmental Change: NASA's Earth Observing System and the Science of ASTER and MODIS, Remote Sensing and Digital Image Processing Series*, B. Ramachandran, C. O. Justice, and M. J. Abrams, Eds. New York, NY, USA: Springer-Verlag, 2011, pp. 549–561.
- [37] Y. Shuai, "Tracking daily land surface albedo and reflectance anisotropy with MODerate-Resolution Imaging Spectroradiometer (MODIS)," Ph.D. dissertation, Boston University, Boston, MA, USA, 2010.
- [38] Z. Wang, C. B. Schaaf, M. J. Chopping, A. H. Strahler, J. Wang, M. O. Román, A. V. Rocha, C. E. Woodcock, and Y. Shuai, "Evaluation of Moderate-Resolution Imaging Spectroradiometer (MODIS) snow albedo product (MCD43A) over tundra," *Remote Sens. Environ.*, vol. 117, pp. 264–280, 2012.
- [39] T. Hwang, C. Song, P. V. Bolstad, and L.E. Band, "Downscaling real-time vegetation dynamics by fusing multi-temporal MODIS and Landsat NDVI in topographically complex terrain," *Remote Sens. Environ.*, vol. 115, no. 10, pp. 2499–2512, Oct. 2011.
- [40] F. Gao, J. G. Masek, R. E. Wolfe, and C. Huang, "Building a consistent medium resolution satellite data set using Moderate Resolution Imaging Spectroradiometer products as reference," *J. Appl. Remote Sens.*, vol. 4, no. 1, pp. 043526-1–043526-22, 2010.
- [41] F. Gao, J. Masek, M. Schwaller, and F. Hall, "On the blending of the Landsat and MODIS surface reflectance: Predicting daily Landsat surface reflectance," *IEEE Trans. Geosci. Remote Sens.*, vol. 44, no. 8, pp. 2207–2218, Aug. 2006.
- [42] J. C. Ju, D. P. Roy, Y. M. Shuai, and C. Schaaf, "Development of an approach for generation of temporally complete daily nadir MODIS reflectance time series," *Remote Sens. Environ.*, vol. 114, pp. 1–20, Jan. 2010.
- [43] T. Hilker, M. A. Wulder, N. C. Coops, N. Seitz, J. C. White, F. Gao, J. G. Masek, and G. Stenhouse, "Generation of dense time series synthetic Landsat data through data blending with MODIS using a spatial and temporal adaptive reflectance fusion model," *Remote Sens. Environ.*, vol. 113, no. 9, pp. 1988–1999, Sep. 2009.
- [44] J. J. Walker, K. M. de Beurs, R.H. Wynnea, and F. Gao, "Evaluation of Landsat and MODIS data fusion products for analysis of dryland forest phenology," *Remote Sens. Environ.*, vol. 117, pp. 381–393, Feb. 2012.
- [45] S. Bhandari, S. Phinn, and T. Gill, "Preparing Landsat image time series (LITS) for monitoring changes in vegetation phenology in Queensland, Australia," *Remote Sens.*, vol. 4, no. 6, pp. 1856–1886, 2012.
- [46] N. C. Coops, T. Hilker, C. W. Bater, M. A. Wulder, S. E. Nielsen, G. McDermid, and G. Stenhouse, "Linking ground-based to satellite-derived phenological metrics in support of habitat assessment," *Remote Sens. Lett.*, vol. 3, no. 3, pp. 191–200, 2012.
- [47] S. Burrows, S. T. Gower, M. K. Clayton, D. S. Mackay, D. E. Ahl, J. M. Norman, and G. Diak, "Application of geostatistics to characterize leaf area index (LAI) from flux tower to landscape scales using a cyclic sampling design," *Ecosystems*, vol. 5, no. 7, pp. 667–679, Nov. 2002.
- [48] S. Ganguly, M. A. Friedl, B. Tan, X. Zhang, and M. Verma, "Land surface phenology from MODIS: Characterization of the Collection 5 global land cover dynamics product," *Remote Sens. Environ.*, vol. 114, no. 8, pp. 1805–1816, Aug. 2010.
- [49] X. L. Zhu, J. Chen, F. Gao, X. Chen, and J. G. Masek, "An enhanced spatial and temporal adaptive reflectance fusion model for complex heterogeneous regions," *Remote Sens. Environ.*, vol. 114, no. 11, pp. 2610–2623, Nov. 2010.
- [50] T. Hilker, M. A. Wulder, N. C. Coops, J. Linke, G. McDermid, J. G. Masek, F. Gao, and J. C. White, "A new data fusion model for high spatial-and temporal-resolution mapping of forest disturbance based on Landsat and MODIS," *Remote Sens. Environ.*, vol. 113, no. 8, pp. 1613–1627, Aug. 2009.
- [51] B. Huang and H. Song, "Spatiotemporal reflectance fusion via sparse representation," *IEEE Trans. Geosci. Remote Sens.*, vol. 50, pp. 3707–3716, Oct. 2012.
- [52] J. G. Masek, E. F. Vermote, N. E. Saleous, R. Wolfe, F. G. Hall, K. F. Huemmrich, F. Gao, J. Kutler, and T.-K. Lim, "A Landsat surface reflectance dataset for North America, 1990–2000," *IEEE Geosci. Remote Sens. Lett.*, vol. 3, no. 1, pp. 68–72, Jan. 2006.
- [53] P. Wang, F. Gao, and J. Masek, "Operational data fusion framework for building frequent Landsat-like images," *IEEE Trans. Geosci. Remote Sens.*, vol. 52, no. 11, pp. 7353–7365, Nov. 2014.
- [54] C. Cammalleri, M. C. Anderson, F. Gao, C. R. Hain, and P. Kustas, "A data fusion approach for mapping daily evapotranspiration at field scale," *Water Resour. Res.*, vol. 49, no. 8, pp. 4672–4686, 2013.
- [55] J. C. Seong, K. A. Mulcahy, and E. L. Usery, "The sinusoidal projection: A new importance in relation to global image data," *Prof. Geograph.*, vol. 54, no. 2, pp. 218–225, May 2002.
- [56] R. R. Sokal and F. J. Rohlf, *Biometry: The Principles and Practice of Statistics in Biological Research*, 4th ed. New York, NY, USA: Freeman, 2012.
- [57] X. Zhang, M. A. Friedl, C. B. Schaaf, A. H. Strahler, and Z. Liu, "Monitoring the response of vegetation phenology to precipitation in Africa by coupling MODIS and TRMM instruments," *J. Geophys. Res.: Atmosph.*, vol. 110, no. D12, p. D12103, Jun. 2005.
- [58] B. Tan, C. E. Woodcock, J. Hu, P. Zhang, M. Ozdogan, D. Huang, W. Yang, Y. Knyazikhin, and R. B. Myneni, "The impact of gridding artifacts on the local spatial properties of MODIS data: Implications for validation, compositing, and band-to-band registration across resolutions," *Remote Sens. Environ.*, vol. 105, no. 2, pp. 98–114, Nov. 2006.
- [59] D. E. Ahl, S. T. Gower, S. N. Burrows, N. V. Shabanov, R. B. Myneni, and Y. Knyazikhin, "Monitoring spring canopy phenology of a deciduous broadleaf forest using MODIS," *Remote Sens. Environ.*, vol. 104, no. 1, pp. 88–95, 2006.
- [60] T. K. Maersperger, P. L. Scaramuzza, L. Leigh, S. Shrestha, K. P. Gallo, C. B. Jenkinson, and J. L. Dwyer, "Characterizing LEDAPS surface reflectance products by comparisons with AERONET, field spectrometer, and MODIS data," *Remote Sens. Environ.*, vol. 136, pp. 1–13, Sep. 2013.
- [61] R. Irish, J. L. Barker, S. N. Goward, and T. Arvidson, "Characterization of the Landsat-7 ETM+ Automated Cloud-Cover Assessment (ACCA) algorithm," *Photogramm. Eng. Remote Sens.*, vol. 72, no. 10, pp. 1179–1188, Oct. 2006.
- [62] L. Oreopoulos, M. Wilson, and T. Várnai, "Implementation on Landsat data of a simple cloud mask algorithm developed for MODIS land bands," *IEEE Trans. Geosci. Remote Sens.*, vol. 8, no. 4, pp. 597–601, Jul. 2011.
- [63] E. Vermote, Landsat Science Team Meeting, Mountain View, CA, USA, Jan. 2010. [Online]. Available: [http://landsat.usgs.gov/science\\_january2010MeetingAgenda.php](http://landsat.usgs.gov/science_january2010MeetingAgenda.php)
- [64] Z. Zhu and C. E. Woodcock, "Object-based cloud and cloud shadow detection in Landsat imagery," *Remote Sens. Environ.*, vol. 118, pp. 83–94, Mar. 2012.
- [65] Landsat data continuity mission (LDCM) Level 1 (L1) data format control book (DFCB), USGS, [April 8, 2013], Aug. 2012. [Online]. Available: <http://landsat.usgs.gov/documents/LDCM-DFCB-004.pdf>
- [66] A. D. Richardson, J. P. Jenkins, B. H. Braswell, D. Y. Hollinger, S. V. Ollinger, and M.-L. Smith, "Use of digital webcam images to track spring green-up in a deciduous broadleaf forest," *Oecologia*, vol. 152, no. 2, pp. 323–334, May 2007.
- [67] A. D. Richardson, B. H. Braswell, D. Y. Hollinger, J. P. Jenkins, and S. V. Ollinger, "Near-surface remote sensing of spatial and temporal variation in canopy phenology," *Ecol. Appl.*, vol. 19, no. 6, pp. 1417–1428, Sep. 2009.
- [68] O. Sonnentag, K. Hufkens, C. Teshera-Sterne, A. M. Young, M. Friedl, B. H. Braswell, T. Milliman, and A. D. J. O'Keefe, "Digital repeat photography for phenological research in forest ecosystems," *Agric. Forest Meteorol.*, vol. 152, pp. 159–177, Jan. 2012.
- [69] A. D. Richardson, R. S. Anderson, M. A. Arain, A. G. Barr, G. Bohrer, G. Chen, J. M. Chen, P. Ciais, K. J. Davis, A. R. Desai, M. C. Dietze, D. Dragoni, S. R. Garrity, C. M. Gough, R. Grant, D. Y. Hollinger, H. A. Margolis, H. McCaughey, M. Migliavacca, R. K. Monson, J. W. Munger, B. Poulter, B. M. Raczka, D. M. Ricciuto, A. K. Sahoo, K. Schaefer, H. Tian, R. Vargas, H. Verbeeck, J. Xiao, and Y. Xue, "Terrestrial biosphere models need better representation of vegetation phenology: Results from the North American Carbon Program Site Synthesis," *Global Change Biol.*, vol. 18, no. 2, pp. 566–584, Feb. 2012.
- [70] J. Dash and P. Curran, "The MERIS terrestrial chlorophyll index," *Int. J. Remote Sens.*, vol. 25, no. 23, pp. 5403–5413, 2004.
- [71] S. Y. Kang, S. W. Running, J.-H. Lim, M. Zhao, C.-R. Park, and R. Loehman, "A regional phenology model for detecting onset of greenness in temperate mixed forests, Korea: An application of MODIS leaf area index," *Remote Sens. Environ.*, vol. 86, no. 2, pp. 232–242, Jul. 2003.
- [72] D. Turner, W. D. Ritts, M. Zhao, S. A. Kurc, A. L. Dunn, S. C. Wofsy, E. E. Small, and S. W. Running, "Assessing interannual variation in MODIS-based estimates of gross primary production," *IEEE Trans. Geosci. Remote Sens.*, vol. 44, no. 7, pp. 1899–1907, Jul. 2006.
- [73] M. White, K. M. De Beurs, K. Didan, D. W. Inouye, A. D. Richardson, O. P. Jensen, J. O'Keefe, G. Zhang, R. R. Neman, W. J. D. Van Leeuwen, J. F. Brown, A. De Wit, M. Schaeppman, X. Lin, M. Dettinger, A. S. Bailey, J. Kimball, M. D. Schwartz, D. D. Baldocchi, J. T. Lee, and W. K. Lauenroth, "Intercomparison, interpretation, and assessment of spring phenology in North America estimated from remote sensing for 1982–2006," *Global Change Biol.*, vol. 15, no. 10, pp. 2335–2359, Oct. 2009.



**Liang Liang** received the Ph.D. degree from the University of Wisconsin-Milwaukee, Milwaukee, WI, USA, in 2009.

He is currently a Bioclimatologist and Assistant Professor with the Department of Geography, University of Kentucky, Lexington, KY, USA. His research interests are focused on understanding the temporal behaviors (phenology) and geographic patterns of plant and vegetation in relation to climate, using remote sensing, bioclimatic models, and field observations.



**Mark D. Schwartz** received the Ph.D. degree from the University of Kansas, Lawrence, KS, USA, in 1985.

He is currently a Phenoclimatologist and Distinguished Professor of Geography with the University of Wisconsin-Milwaukee Milwaukee, WI, USA. His research interests are focused on plant phenology–lower atmosphere interactions during the onset of spring in midlatitudes, detecting climatic change, and assessing the vegetation condition with remote sensing imagery.



**Zhuosen Wang** received the B.S. degree in geography from Beijing Normal University, Beijing, China, and the Ph.D. degree in geography from Boston University, Boston, MA, USA, in 2003 and 2011, respectively.

He has been a NASA Postdoctoral Fellow with the NASA Goddard Space Flight Center, Greenbelt, MD, USA. His areas of interest include the following: 1) monitoring of the high-latitude snow melt and energy balance; 2) modeling and evaluation of the anisotropic characteristics and albedo of the

land surface; 3) monitoring of the vegetation phenology and climate change; 4) canopy structure estimation using optical remote sensing and lidar; and 5) carbon and energy cycle and flux simulation using a regional land surface model in coastal areas.



**Feng Gao** received the B.A. degree in geology and the M.E. degree in remote sensing from Zhejiang University, Hangzhou, China, in 1989 and 1992, respectively, the Ph.D. degree in geography from Beijing Normal University, Beijing, China, in 1998, and the M.S. degree in computer science from Boston University, Boston, MA, USA, in 2003.

From 1992 to 1998, he was a Research Assistant with the Chinese Academy of Sciences, Nanjing, China. From 1998 to 2004, he was a Research Associate Professor with the Department of Geography

and a Researcher with the Center for Remote Sensing, Boston University. From 2004 to 2011, he was a Research Scientist with the Earth Resources Technology, Inc., and the NASA Goddard Space Flight Center. Since 2011, he has been a Research Scientist with the Hydrology and Remote Sensing Laboratory, USDA Agricultural Research Service. His recent research interests include remote sensing modeling, multisensor data fusion, and vegetation biophysical parameter retrieving for crop and ecosystem condition monitoring.

Dr. Gao has been a member of the Landsat Science Team since 2006.



**Crystal B. Schaaf** (M'92) received the S.B. and S.M. degrees in meteorology from the Massachusetts Institute of Technology, Cambridge, MA, USA, in 1982, the M.L.A. degree in archaeology from Harvard University, Cambridge, in 1988, and the Ph.D. degree in geography from Boston University, Boston, MA, in 1994.

She is currently a Professor with the School for the Environment, University of Massachusetts, Boston. She is a Science Team Member working on the development and use of operational products from the

MODerate Resolution Imaging Spectroradiometer (MODIS) on board NASA's Terra and Aqua polar-orbiting space platforms. She is also a Science Team Member for the Visible Infrared Imaging Radiometer Suite sensor on board the new weather and environmental Suomi National Polar-orbiting Partnership satellite and for the new Landsat 8 environmental satellite. Her early research focused on the use of remote sensing in automated cloud analyses and the detection of initiating convective clouds. Her current interests include modeling reflectance anisotropy and albedo and using remote sensing data to reconstruct and monitor the reflectance characteristics, vegetation phenologies, and disturbance histories of various land and coastal ecosystems. More recently, she has been involved in the development and use of ground-based lidar systems to characterize biomass and vegetation structure.

**Bin Tan** received the B.S. degree in geography and the M.S. degree in remote sensing and GIS from Peking University, Beijing, China, in 1998 and 2001, respectively, and the Ph.D. degree in geography from Boston University, Boston, MA, USA, 2005.

From 2005 to 2007, he was a Research Associate with the Department of Geography, Boston University. He joined the NASA Goddard Space Flight Center, Greenbelt, MD, USA, in 2007. His recent research interests include temporal data analysis, retrieving biophysical parameters from satellite data, land cover classification with high-resolution satellite data, and assessment of the geolocation accuracy of satellite data.



**Jeffrey T. Morissette** received the Ph.D. degree from the North Carolina State University, Raleigh, NC, USA, in 1997.

He is currently the Director of the DOI North Central Climate Science Center; which is working to provide the best available climate science to natural and cultural resource managers in the region. Some of his existing research includes large-scale species habitat mapping and work on land surface phenology estimates from satellite data.



**Xiaoyang Zhang** received the B.A. degree in geography from Peking University, Beijing, China, in 1984, the M.S. degree from the Chinese Academy of Sciences (CAS), Nanjing, China, in 1991, and the Ph.D. degree in remote sensing from King's College London, London, U.K., in 1999.

He was a Research Assistant Professor with the Institute of Hydrobiology, CAS; a Research Associate Professor with the Institute of Geodesy and Geophysics, CAS, from 1984 to 1995; and a Research Associate and Research Assistant Professor

with the Department of Geography, Boston University, Boston, MA, from 1999 to 2005. As a Senior Research Scientist with the Earth Resources Technology, Inc. (2005–2012), and an Associate Research Scientist with the Earth System Science Interdisciplinary Center, University of Maryland, College Park, MD, USA (2012–2013), he worked at the National Oceanic and Atmospheric Administration/National Environmental Satellite, Data, and Information Service through a contract. Since August 2013, he has been an Associate Professor/Senior Research Scientist with the Geospatial Sciences Center of Excellence, South Dakota State University, Brookings, SD, USA. His research interests include satellite remote sensing of vegetation seasonality and biomass burning emissions, climate–vegetation interaction, and land surface modeling.